Demonstration of light recycling in a Michelson interferometer with Fabry–Perot cavities

Peter Fritschel, David Shoemaker, and Rainer Weiss

We describe the first experimental demonstration of light recycling of a Michelson interferometer with Fabry–Perot cavities in the arms of the interferometer. Light recycling is a technique for efficiently using the light in long-baseline interferometers, such as those being proposed for the detection of gravitational radiation. An increase in the interferometer circulating power by a factor of 18 is observed, which is in good agreement with the expected gain given the losses in the system. Several phenomena associated with this configuration of coupled optical cavities are discussed.

Key words: Interferometry, Michelson, Fabry–Perot, techniques for gravitational radiation detection, light recycling, coupled cavities.

I. Introduction

The development of prototype laser interferometers for the detection of gravitational radiation has led to the ability to detect differential displacements on the order of 10^{-18} m/$\sqrt{\text{Hz}}$ (10^{-18} m of rms motion in a 1-s integration time).[1] These interferometers sense a differential phase shift of the laser light in the two arms of a Michelson interferometer through the intensity change this phase shift produces when the two beams are recombined at the beam splitter. The output signal is proportional to the optical power in the interferometer for a given phase shift. The phase shift produced by a given mirror displacement can be increased by arranging for the light to make multiple passes in each arm, using either a resonant Fabry–Perot cavity or an optical delay line. Proposed techniques for further signal increase, capitalizing either on an increase in the optical power or an increase in the phase shift, include power, detuned, resonant, and dual recycling.[2–5] In each case the smallest detectable signal is limited, at best, by photon-counting statistics; without the use of squeezed states of light, we find that the equivalent phase noise caused by these quantum fluctuations (expressed as spectral density ϕ_{noise} in units of rad/Hz$^{1/2}$ is equal to

$$\phi_{\text{noise}} = (2h\upsilon/\eta P)^{1/2}, \tag{1}$$

where h is Planck's constant, υ is the light frequency, η is the photodetector efficiency, and P is the bright fringe optical power. The concepts of power recycling[6] and dual recycling[7] have recently been demonstrated on small-scale fixed-mass interferometers with simple one-bounce mirrors in the arms. As part of the research and development program in support of the Caltech/MIT Laser Interferometer Gravitational Wave Observatory (LIGO) project,[8] we have built a small fixed-mirror interferometer with Fabry–Perot cavities in the arms. Here we report on the first experimental demonstration of power recycling of a such a system. To illuminate any practical difficulties with such a complex, coupled-cavity system and to verify the theory of recycling, this experiment is intended as a proof of principle.

II. Simplified Theory of Power Recycling

The basic optical arrangement for power recycling is shown in Fig. 1(a). The average power at the antisymmetric output of a Michelson interferometer is equal to

$$P_{\text{anti}} = \tfrac{1}{2} P_0[1 - C\cos(\bar{\phi}_d)], \tag{2}$$

where $\bar{\phi}_d$ is the average phase difference between the two arms and $P_0 = P_{\text{max}} + P_{\text{min}}$, where P_{max} is the output power on the bright fringe ($\bar{\phi}_d = \pi$) and P_{min} is the output power on the dark fringe ($\bar{\phi}_d = 0$). The contrast is $C = (P_{\text{max}} - P_{\text{min}})/(P_{\text{max}} + P_{\text{min}})$. In principle the interferometer could be operated at any point on this fringe. To achieve the best signal-to-noise ratio in a real system, however, the optimal place to operate is at $\bar{\phi}_d = 0$, i.e., the dark fringe. The fluctuating phase difference, $\phi_d(f)$, can then be measured either by differentially phase modulating the light in the two arms and then demodulating the output signal,[9] or by interfering the output field with a phase-modulated reference field (i.e., external modulation).[6,10] In a well-balanced interferometer, dark fringe operation implies that nearly all the light (to the extent that power is not lost because of imperfect

The authors are with the Department of Physics and Center for Space Research, Massachusetts Institute of Technology, Cambridge, Massachusetts 02139.

Received 10 June 1991.
0003-6935/92/101412-07$05.00/0.

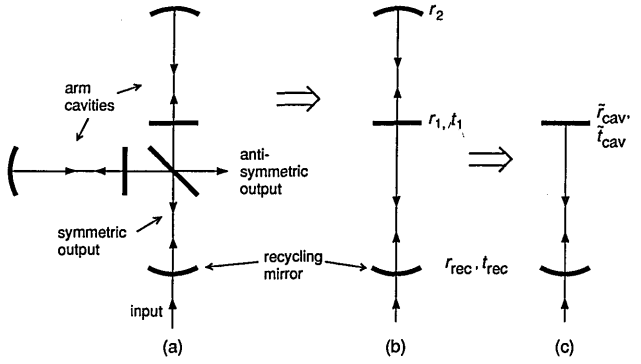

Fig. 1. (a) Optical elements of a recycled Michelson interferometer with Fabry–Perot cavities in the arms. (b) When the interferometer is operating at the dark fringe of the antisymmetric output, the two arms and beam splitter are modeled by one arm cavity, creating a three-mirror cavity. (c) The arm cavity is then modeled by a single mirror, having reflection and transmission coefficients of a Fabry–Perot cavity. The tilde denotes a complex quantity.

optics) exits through the symmetric output and travels back toward the light source. From the standpoint of the input laser beam, the interferometer looks like a mirror of reflectivity somewhat less than unity because of losses in the optics and an imperfect contrast. The power circulating in the interferometer can then be increased by making an optical cavity, with a recycling mirror at the input of the interferometer as the cavity-input mirror and with the interferometer forming the rear mirror [Fig. 1(b) and 1(c)].

For a simple two-mirror Fabry–Perot cavity on resonance, the ratio of the internal power to the input power is

$$P_{int}/P_0 = \frac{T_1}{[1-(R_1R_2)^{1/2}]^2} = \frac{T_1}{\{1-[(1-A_1-T_1)(1-A_2)]^{1/2}\}^2}, \quad (3)$$

where T_i, R_i, and A_i are the power transmission, reflection, and loss coefficients respectively of the input mirror ($i = 1$) or the rear mirror ($i = 2$). Any transmission of the rear mirror is included in the loss A_2, so $1 - R_2 = A_2$. Applied to a recycled interferometer, T_1 is the transmission of the recycling mirror, R_2 is the reflectivity, and A_2 is the loss of the interferometer operating on the dark fringe. The ratio P_{int}/P_0 is dubbed the recycling gain, G_{rec}. For a given R_2 and input-mirror loss A_1, the ratio P_{int}/P_0 is a maximum for

$$T_1 = (1-A_1)[1-R_2(1-A_1)]. \quad (4)$$

With this simple Fabry–Perot model for recycling, we find that the maximum increase in the interferometer circulating power is then

$$G_{rec}^{max} = P_{int}^{max}/P_0 = \frac{1}{A_2 + A_1/(1-A_1)} \approx \frac{1}{A_2 + A_1}. \quad (5)$$

The basic result is that the maximum recycling gain is equal to 1/(total loss).

Power recycling thus gives an increase in the output signal by a factor of G_{rec} and a corresponding reduction of the equivalent phase noise by a factor of $\sqrt{G_{rec}}$, as shown in Eq. (1). The signal, proportional to the phase difference between the arms, exits directly through the antisymmetric output; it is therefore not recycled and experiences only a single-arm storage time. The consequence is that the frequency response of the output signal to a phase difference in the arms is not affected by power recycling: the signal-to-noise ratio is increased by a factor of $\sqrt{G_{rec}}$ without changing the band width of the interferometer. For a detailed discussion of the frequency response of this and other interferometer configurations, refer to Ref. 5.

Two further points are worth noting. For the case of a single mirror or delay line in each arm, the interferometer, as viewed from the symmetric side of the beam splitter, does indeed look like a simple mirror. It can be (conceptually) replaced, in the limit of perfect contrast, with a mirror of amplitude reflection coefficient $r_{equiv} = (r_{arm})^b$, where r_{arm} is the amplitude reflection coefficient of an arm mirror and b is the number of bounces in an arm. For the configuration with cavities in the arms, however, the interferometer must be replaced with a mirror that has the more complicated amplitude reflection coefficient of a Fabry–Perot cavity. The model for the recycled interferometer is now a three-mirror cavity, as shown in Fig. 1(b). This cavity leads to some interesting mode-coupling phenomena, which will be discussed in more detail in Section V.

The other point is that in the Fabry–Perot configuration, in order for the loss in the arm cavities to be small, the transmission of the cavity-input mirrors must be much greater than the mirror loss. To investigate recycling with a significant power gain, we have chosen a cavity finesse as high as possible within the limitation of keeping the cavity losses low. For the cavity loss to be not much greater than a few percent, the mirror loss of ~ 100 parts in 10^6 in this experiment requires that the input-mirror transmission be at least a few percent.

III. Description of Apparatus

We have carried out our work on a small-scale, fixed-mirror interferometer in air; this is a much simpler system than the in-vacuum, suspended-mirror design required for a gravity wave antenna, and it allows us to concentrate on the optical configuration. This configuration requires that noise measurements must be made at frequencies >20 kHz, where ambient acoustical and mechanical excitations are much reduced, and that the servo systems must be tailored for types and levels of excitation not found in an in-vacuum, suspended design. The optical and servo system that we used is depicted in Fig. 2. The mechanical and optical construction is very similar to the apparatus described in detail in Ref. 11. A main difference from that description is that our laser light, a single frequency at 514.5 nm produced by a Spectra-Physics 2020 Ar^+ laser, is frequency stabilized to a separate reference cavity (length 30 cm, finesse 200) rather than to one of the interferometer arm cavities.

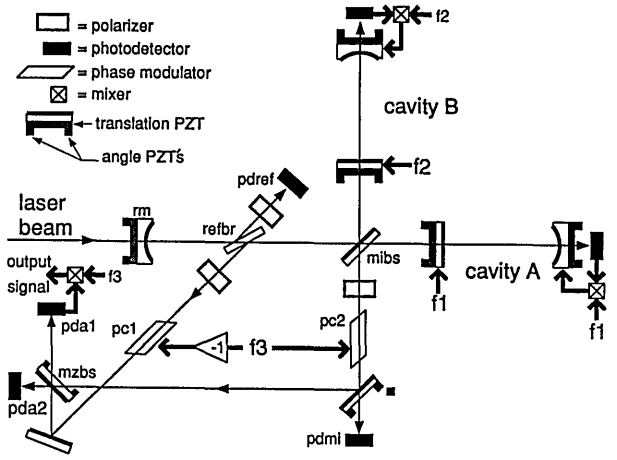

Fig. 2. Experimental arrangement.

Each interferometer mirror is mounted on a piezoelectric transducer (PZT) that allows ~1 μm of translational control. In addition, each mirror is held in a mount outfitted with two PZT's, which provide ~3 mrad of remote alignment control in each of the two pertinent angular degrees of freedom.

Each arm cavity is 47 cm long and is constructed of a flat, 2.8% transmission input mirror and a 1-m radius of curvature, maximum reflectivity rear mirror; the finesse is thus ~220 and the linewidth is 1.4 MHz. These mirrors are special low-loss mirrors that are made of superpolished substrates with ion-beam sputtered dielectric coatings. The average loss per arm-cavity mirror is about 1.2×10^{-4}; this loss leads to an on-resonance loss on reflection of ~3.3% for each cavity. The fraction of the input power coupled into the TEM_{00} mode of each cavity (without recycling) is $\sim M = 95\%$. To within ±5%, we measure no difference in the matching, finesse, or losses of the two cavities. We are able to measure these properties of the individual cavities with the recycling mirror in place by merely misaligning the recycling mirror so that there is no interference in the optical path between the recycling mirror and the interferometer. The alignment of the beam to the interferometer is not significantly changed by this recycling-mirror motion. The fact that we do not have to remove the recycling mirror means that measurements of power gain and loss can all be made in a short period of time.

The cavity made up of the recycling mirror, rm; the mirror formed by the two arm-input mirrors is referred to as the recycling cavity. The recycling mirror has a 1-m radius of curvature and is placed 53 cm from the arm-input mirrors, so the TEM_{00} mode in the recycling cavity is matched, at the arm-input mirrors, to the TEM_{00} mode in the arm cavities. Ideally, the transmission of the recycling mirror should be equal to the total loss in the interferometer; the closest match available to us was an ordinary commercial laser mirror of 8.3% transmission and 0.3% estimated loss. The recycling mirror is also provided with PZT controls for one translational and two angular degrees of freedom.

Each arm cavity is held on resonance with a lock-in detection method: The length of a cavity is modulated with the input-mirror PZT at a frequency (f_m) lower than the cavity band width; the light transmitted by the cavity is detected and this signal is demodulated at f_m; the resulting error signal is applied to the rear-mirror PZT of the cavity. Different length-modulation frequencies are used for the two cavities—f_1 = 70 kHz for cavity A and f_2 = 90 kHz for cavity B—so that the two servo systems do not couple to one another (see Section V on cavity-coupling phenomena). The Michelson antisymmetric output power is monitored with photodiode pdmi. The fringe operating point is controlled by using the PZT's to manually adjust the positions of the arm cavities with respect to the Michelson beam splitter. The setup is stable enough so that a servo control to keep the output on a dark fringe is not needed. Servo control of the recycling cavity length is also not needed, as we will explain below.

IV. Measurements

Measurements are made of the signal $\phi_d(f)$ and the noise at the antisymmetric output and of the optical power sampled at three points in the interferometer; in the recycling cavity; in the arm cavities; and at the antisymmetric output (giving a measure of the contrast).

The output signal from the interferometer is detected with the external modulation technique[6]; many of the experimental techniques in the realization of this scheme were first discussed by Schilling and Schnupp.[12] A small fraction ($\approx 2.5 \times 10^{-4}$) of the intrarecycling cavity power is reflected by a near-Brewster's-angle beam splitter, refbr, and forms the reference arm of a Mach–Zehnder interferometer. By taking the reference beam from the Michelson beam splitter symmetric output inside the recycling cavity, we can make the path lengths of the reference beam and the Michelson output beam the same. The Mach–Zehnder relative phase is $\phi^{MZ} = \phi_{ref} - \phi_{MI}$, where the phases of the reference beam (ϕ_{ref}) and the Michelson output beam (ϕ_{MI}) are defined with respect to their common phase at the Michelson beam splitter. The measurement is transferred to a high frequency, where the laser power is shot-noise limited, by modulating the phase ϕ^{MZ} at f_3 = 5.38 MHz in the arms of the Mach–Zehnder interferometer with Pockels cells pc1 and pc2. After the reference beam and the Michelson output beam are combined on the 50–50 Mach–Zehnder beam splitter mzbs, the photodetector *pda*1 output is demodulated at f_3 to retrieve the Michelson phase-difference signal.

The static Mach–Zehnder relative phase, ϕ_0^{MZ}, is controlled with a bias voltage on the Pockels cells so that the Michelson signal at 70 (or 90) kHz, as indicated by the demodulated output of pda1, is a maximum. The Michelson signal detected by the Mach–Zehnder interferometer is proportional to $\sin(\phi_0^{MZ})$, so when the system has maximum sensitivity to the Michelson phase difference ($\phi_0^{MZ} = \pi/2$), this sensitivity depends on the Mach–Zehnder relative phase only in second order. The combination of

this insensitivity and the mechanical stability of the system means that accurate measurements of the signal can be made without servo controlling ϕ^{MZ}.

When the contrast is less than one, we find that a signal with first-order sensitivity to ϕ^{MZ} does remain, but this signal is smaller than the Michelson signal by a factor of $\sim[2/(1 - C_{00})]^{1/2}$, where C_{00} is the Michelson contrast for the TEM_{00} component of the antisymmetric output beam. Inspection of the spatial intensity pattern at the antisymmetric port of the interferometer shows that the majority of the contrast defect in our system is caused by wave-front distortion: The light at the dark fringe is dominated by modes of higher order than the TEM_{00} mode. Thus the measured contrast $C < C_{00}$ can be used to obtain an upper limit for this factor; this inequality gives $[2/(1 - C_{00})]^{1/2} \geq 80$.

The system is brought into angular alignment and resonance in steps. First, with the recycling mirror misaligned, we align the two arm cavities for maximum coupling to the TEM_{00} modes. Then, with the arm cavities locked on resonance, we adjust the Michelson phase to the dark fringe and give the arm mirrors further small alignments to achieve the minimum dark fringe. We then bring the recycling mirror into rough alignment (the arm cavities do not remain resonant for this step). With an arbitrary initial length of the recycling cavity, we adjust the two arm-cavity lengths for resonance and hold them there with the servos. The recycling-cavity length is then adjusted for resonance in the recycling cavity, and each mirror is aligned for maximum power in the system. Because of the phase shift on reflection from an arm cavity (π rad on resonance, ≈ 0 rad off resonance), the recycling-cavity resonance length depends on the length of the arm cavities.

Measurements of the recycling-power gain were made for three configurations of the Michelson interferometer: a simple Michelson using only the input mirrors of the arm cavities (the light paths to the rear mirrors are blocked); the Michelson with the two Fabry-Perot cavities in the arms; and the asymmetric Michelson, with a Fabry-Perot cavity in one arm and a simple mirror (the second arm-cavity input mirror) in the other. Photodiode pdref monitors the signal reflected from refbr and gives a measure of the input power when the recycling mirror is misaligned and a measure of the power gain when the system is recycled. The polarizer between the reference splitter *refbr* and the photodiode *pdref* ensures that only light in the (horizontal) polarization of the input beam is detected; the polarizers on the other side of the reference splitter and at the antisymmetric output serve the same purpose.

In the simple Michelson case, we observe the maximum power gain to be $G_{rec} = 19.5$. To compare this gain with the expected value, we make an accounting of the measured and estimated loss as shown in Table I.

The estimated losses are based on experience with other optics that have the same kind of dielectric coating. The factor of 1/2 for the round-trip loss of the beam splitter antireflection-coated surface accounts for the fact that this loss occurs only in one arm; the factor of 2 in the loss per pass of the reference beam splitter accounts for the two surfaces of the splitter. The contrast defect refers to the average fractional power coming out the antisymmetric port of the Michelson beam splitter. Using the values of $T_1 = 8.3\%$, $A_1 = 0.3\%$, and $A_2 = 4.03\%$ in Eq. 3 gives us an expected power gain of 20.6. The measured factor of 19.5 is the ratio of the recycling-cavity internal power to the total input power. If we correct for the fraction of the input power that is in the TEM_{00} mode of the cavity, $M = 0.95$, we find that the measured increase in the TEM_{00} mode is $G_{rec}^{TEM_{00}} = 19.5/0.95 = 20.5$; the agreement between the expected and measured values is quite good.

Table I. Losses for the Recycled Simple Michelson Interferometer

Loss Element	Loss per Pass (%) [a]	Round-Trip Loss (%)
Cavity input mirror: Transmission	2.8 (m)	2.8
Cavity input mirror: Reflection from antireflection-coated surface	0.2 (m)	0.4
Beam splitter: 50–50 surface	0.3 (e)	0.6
Beam splitter: antireflection-coated surface	0.15 (e)	(1/2) × 0.3
Reference beam splitter	2 × 0.015 (m)	0.06
Recycling mirror	0.3 (e)	0.3
Contrast defect	0.02 (m)	0.02
Total round-trip loss		4.33

[a] m, Measured; e, estimated.

For the configuration with Fabry-Perot cavities in the arms of the Michelson interferometer, we find the maximum observed gain to be $G_{rec}^{TEM_{00}} = 18.0$, which is corrected for the recycling-cavity TEM_{00} mode-matching of $M = 0.95$. $G_{rec}^{TEM_{00}}$ is the ratio of the recycling-cavity internal power to the input power; the power in the arm cavities, as measured by the cavity transmissions, also increases by this factor (to within ±5%). In this case we show the loss accounting in Table II.

The effect of the slightly differing loss in the two cavities has been approximated by using the average cavity loss for the round-trip loss from the cavities. The expected value of the recycling gain, with $T_1 = 8.3\%$, $A_1 = 0.3\%$, and $A_2 = 4.6\%$ in Eq. 3, is $G_{rec}^{predicted} = 18.9$. With these losses the recycling gain for the optimal recycling mirror, $T_1 \approx A_1 + A_2 = 4.9\%$, would be 20.4; the penalty for using a recycling mirror with a transmission somewhat higher than optimum is not high.

In each configuration, we measure the 70- (or 90-) kHz signal (ϕ_d) with the Mach–Zehnder interferometer. The increase in the signal with recycling is found to be equal, within ±5%, to the increase in the recycling-cavity internal power, verifying that the signal does increase with the circulating power. The absolute signal size, given the applied mirror motion,

Table II. Losses for the Recycled Fabry–Perot Arm Michelson Interferometer

Loss Element	Loss per Pass (%) [a]	Round-Trip Loss (%)
Cavity A reflection	3.1 (m)	
Cavity B reflection	3.4 (m)	1/2(3.1 + 3.4)
Cavity A and B input mirrors: reflection from antireflection-coated surface	0.2 (m)	0.4
Beam splitter, mibs: 50–50 surface	0.3 (e)	0.6
Beam splitter, mibs: antireflection-coated surface	0.15 (e)	1/2 × 0.3
Beam splitter, refbr	(2)×0.025 (m)	0.1
Recycling mirrow	0.3 (e)	0.3
Contrast defect	0.1 (m)	0.1
Total round-trip loss		4.9

[a] m = measured; e, estimated.

the intensities in the Mach–Zehnder interferometer, and the Mach–Zehnder modulation depth, is compared with the level predicted by the theory of Ref. 6. In each case the measured signal is found to be less than the predicted level by a factor of ~1.2. This is a reasonable agreement, considering the ~10% uncertainties in the above parameters. The signal is also found to increase proportionally with $J_1(m)$ up to the maximum modulation index we can achieve, which is $m = 0.83$ (the maximum of J_1 occurs for $m = 1.82$). The sensitivity to the Mach–Zehnder phase, ϕ^{MZ}, is measured to be 200–1000 times less than the sensitivity to the Michelson phase, which is consistent with the lower limit calculated above.

The output noise is also examined with the Mach–Zehnder interferometer by measuring the power spectrum of the output of photodetector pda1. For the recycled Fabry–Perot Michelson interferometer, we find that the output noise is much larger than the contribution caused by the shot noise and that it is limited by various unidentified mechanical resonances. In addition, relatively large low-frequency signals saturate the photodetector for Mach–Zehnder modulation depths in excess of $\sim m = 0.025$. It is clear that a fixed-mass, in-air system is not suitable for detailed noise studies.

The results of the asymmetric Michelson interferometer, consisting of a Fabry–Perot in one arm and a simple mirror (the cavity-input mirror) in the other, address the question of how the interferometer contrast changes with recycling. In the nonrecycled asymmetric configuration, the contrast is poor for the following reason. Light in the cavity arm that does not couple into the cavity does not experience the additional cavity π-rad phase shift, but in the simple-mirror arm all the light experiences the same phase shift at the mirror. Therefore, at the antisymmetric output, the higher-order modes from the two arms constructively interfere at a Michelson path-length difference from which the TEM_{00} modes destructively interfere. The contrast we measure in the nonrecycled case is $C = 0.77$, which corresponds to ~10% of the light contained in higher-order modes. The recycling cavity rejects these higher-order modes to some degree when this system is recycled. The contrast becomes $C = 0.98$. If this contrast defect is still caused by higher-order modes, this implies that the mode matching of the recycling-cavity light into the arm cavities is $M = 0.99$.

The contrast also improves for the symmetric arm configurations when the system is recycled. For a contrast near unity, we find that the fractional power lost at the antisymmetric output is $A_C \approx (1 - C)/2$. The measured loss in our system for the various configurations is as follows. Simple MI (Michelson): $A_C = 5.6 \times 10^{-4}$; recycled simple MI: $A_C = 1.5 \times 10^{-4}$; FPMI (Michelson with cavities in the arms): $A_C = 1.7 \times 10^{-3}$; recycled FPMI: $A_C = 3.4 \times 10^{-4}$. The figures refer to the minimum power detected with *pdmi*. In the FPMI configurations, large residual low-frequency signals ($f \sim 100$ Hz) make the average power (averaged over ~0.1 s) on *pdmi* ~3–4 times the minimum. It is the average power loss that appears in the loss accounting in Tables I and II as the contrast defect. The fractional power lost through the antisymmetric output decreases by a factor of 4–5 when the system is recycled for both the simple MI and the FPMI. We are still investigating the mechanism to explain this phenomenon.

V. Cavity Coupling

As was mentioned in Section II, the recycled Fabry-Perot arm interferometer can be modeled by a three-mirror cavity, as shown in Fig. 1(b). It is convenient to view this as a two-mirror cavity, formed by replacing the middle and rear mirrors (i.e., the arm cavity) with a mirror that has the amplitude reflection and transmission coefficients of a Fabry-Perot cavity, $(\tilde{r}, \tilde{t})_{cav}$ [Fig. 1(c); the tilde denotes a complex quantity]:

$$\tilde{r}_{cav}(\theta) = \frac{r_1 - r_2(r_1^2 + t_1^2)\exp i\theta}{1 - r_1 r_2 \exp i\theta}, \quad \tilde{t}_{cav}(\theta) = \frac{t_1 t_2 \exp i\theta/2}{1 - r_1 r_2 \exp i\theta}, \tag{6}$$

where r_i (t_i) is the amplitude reflection (transmission) coefficient of the input mirror ($i = 1$) or the rear mirror ($i = 2$), and the independent parameter $\theta = 2\omega l/c$ is a dimensionless expression for the optical frequency deviation from the cavity resonance. In this expression, ω is the optical frequency in radians per second, l is the cavity length, and c is the speed of light. An imperfect contrast can be accounted for by multiplying $\tilde{r}_{cav}$ by a factor of < 1. The three-mirror cavity then consists of an input (recycling) mirror characterized by r_{rec} and t_{rec}, and a rear mirror characterized by $\tilde{r}_{cav}$ and $\tilde{t}_{cav}$. In general the resonance properties of such a cavity are quite complex, with the mode losses depending on the field distribution between the two cavities; see Ref. 13 for a discussion. For example, the ratio of the field inside the recycling cavity to the input field is

$$E_{rec}/E_0 = \frac{t_{rec}(1 - r_1 r_2 \exp i\theta_c)}{1 - r_1 r_2 \exp i\theta_c + r_{rec}(r_1 - r_2(r_1^2 + t_1^2)\exp i\theta_c)\exp i\theta_r}, \tag{7}$$

where $\theta_c = 2\omega l_{cav}/c$ and $\theta_r = 2\omega l_{rec}/c$. The double resonance condition of recycling corresponds to $\theta_c = 2n\pi$ and $\theta_r = 2m\pi$.

The linewidth of the combined cavity, $\Delta\nu_{rec}$, is defined as the full width at half maximum of the recycling-cavity internal power curve as a function of the optical frequency. The pole frequency of a cavity, the point where the magnitude of the frequency response is down by 3 dB and the phase is at −45 deg, occurs at half the cavity linewidth. When the loss is dominated by the arm cavity and the optimum recycling mirror has been chosen (T_1 = loss), some manipulation of Eq. (7) gives

$$\Delta\nu_{rec} \approx \Delta\nu_{cav}(1 - R_{cav})/2 = \Delta\nu_{cav}/2G_{rec}, \tag{8}$$

where $\Delta\nu_{cav}$ is the linewidth (full width, half maximum) of the isolated arm cavity and $R_{cav} = |\tilde{r}_{cav}(0)|^2$ is the power reflection coefficient of the arm cavity on resonance. This is a much narrower linewidth than that of an arm cavity. For our system, a numerical solution of Eq. (7) gives the combined linewidth as $\Delta\nu_{rec} \approx 50$ kHz, compared with the individual arm-cavity linewidth of $\Delta\nu_{cav} \approx 1.4$ MHz. The 70- and 90-kHz modulation frequencies of the arm-cavity lengths are much lower than the 700-kHz pole frequency of an isolated arm cavity, so when the system is not recycled the 70- and 90-kHz sidebands have nearly zero phase shift with respect to the carrier. With recycling the pole frequency of the system becomes ~25 kHz. The 70- and 90-kHz sidebands thus acquire an additional phase shift of about 70 deg because of the coupled-cavity response. The consequence is that the servos require a compensating shift in the phase of each lock-in local oscillator.

The addition of the recycling mirror also couples the two arm cavities to one another. For example, fluctuations in the length of cavity A produce fluctuations in the amplitude and phase of the field reflected from cavity A. Because of the recycling mirror, these fluctuations appear in the input field to cavity B, and thus also in the reflected and transmitted fields of cavity B. Our cavity-length modulation servos work by holding to zero the signal at f_m transmitted by each cavity. If the cavities were modulated at the same frequency and one of the cavities, e.g., A, were slightly off resonance, some of the signal at f_m transmitted through cavity B would be caused by the field reflected from cavity A. The cavity B servo would misinterpret this signal and cavity B would not necessarily be held to a local maximum of the internal power. We thus have to modulate the two arm cavities at different frequencies so that length changes of cavity A will not be interpreted by the cavity B servo as length changes of cavity B. Note that laser amplitude noise can corrupt the servos in the same way, but the amplitude noise of the laser at 70 and 90 kHz is not large enough to be a problem.

The action of the arm servos revealed a further coupling between the recycling-cavity length and the arm-cavity lengths. Consider the case of the three-mirror cavity, Fig. 1(b), initially at the double resonance condition, $\theta_c = 2n\pi$ and $\theta_r = 2m\pi$. This is the point at which the power coupled into the arm cavity, and thus the power transmitted through the system, is a (global) maximum. If the recycling cavity is not resonant, so that $\theta_r = 2m\pi + \Delta\theta_r$, the power transmitted through the system is maximized for $\theta_c \neq 2n\pi$, though at a lower level than the double resonance condition, the explaination is as follows:

With respect to the input field E_0, the field transmitted through the coupled cavities is

$$E_T/E_0 = \frac{t_{rec}t_1t_2 \exp i(\theta_r + \theta_c)/2}{1 + r_{rec}r_1 \exp i\theta_r - r_1r_2 \exp i\theta_c - r_{rec}r_2(r_1^2 + t_1^2)\exp i(\theta_r + \theta_c)}. \tag{9}$$

The magnitude of the transmitted field is a maximum for an arm-cavity length of

$$\theta_c = \tan^{-1}\left\{\frac{-r_{rec}t_1^2 \sin\theta_r}{r_1[1 + r_{rec}^2(r_1^2 + t_1^2)] + r_{rec}(2r_1^2 + t_1^2)\cos\theta_r}\right\}. \tag{10}$$

If $\theta_r = 2m\pi$ or $r_{rec} = 0$, this shows that the transmitted power is a maximum at $\theta_c = 2n\pi$, as it must be. In general, however, the maximum occurs for $\theta_c \neq 2n\pi$. A numerical examination of Eq. (10), using the values of r_1 and t_1 for our system, shows that when r_{rec} is not near zero and $\Delta\theta_r \ll 1$, the maximum transmission occurs at a θ_c for which the phase on reflection from the arm cavity (in addition to the on-resonance phase shift of π rad) is very nearly $-\Delta\theta_r$.

That is, if the arm servo is holding the arm cavity to a maximum in transmitted power, than the round-trip phase in the recycling cavity (propagation phase plus arm-cavity reflection phase) is essentially restored to $2m\pi$. The resulting decrease in the power in the arm cavity is determined by the isolated arm-cavity linewidth rather than by the much narrower $\Delta\nu_{rec}$, because the recycling cavity remains resonant. For our system, with a constant arm-cavity length of $\theta_c = 2n\pi$, the half-power points of the transmitted light, Eq. (9), occur at a deviation from the resonant recycling-cavity length ($\theta_r = 2m\pi$) of $\Delta\theta_r = \pm 0.048$ rad. With the arm cavity under servo control, so that the arm-cavity length is given by Eq. (10), the half-power points of the transmitted light occur for $\Delta\theta_r = \pm 1.75$ rad. The combination of this compensation of recycling-cavity length fluctuations by the arm-cavity servo and the mechanical stability of the system means that accurate measurements (to within ±1%) of the signal and power levels at the double resonance condition can be made without actively stabilizing the recycling-cavity length.

VI. Scaling the Optical Configuration

As a techique for increasing the position sensitivity of an interferometer in the practically accessible gravity wave band (100 Hz $\lesssim f \lesssim$ 10 kHz), power recycling only makes sense on a large-scale (several kilometer arm lengths) interferometer. The reasoning is as follows. To optimize the position sensitivity, we should

store the light in each arm for a time that is comparable with half the period of the lowest frequency gravity wave, f_0, the interferometer is designed to detect. For prototype-scale interferometers (arm lengths tens of meters or less), this requirement leads to a large number ($\geq 10^4$) of equivalent bounces in the arms. For a Fabry-Perot interferometer of length l, an input-mirror intensity transmission T_1, and a total mirror loss A, this requirement translates into choosing the cavity-energy storage time, $\tau_{st} \approx 2l/c(T_1 + A)$, to be $\tau_{st} = 1/4\pi f_0 \approx 1$ ms. This time can be achieved by making the arm input-mirror transmission very low, but then, given the loss in current state-of-the-art mirrors (10–100 parts in 10^6), a majority of the light would be lost (absorbed or scattered) in the arms. In this case power recycling cannot give a significant increase in power. In a full-scale interferometer (arm lengths of a few kilometers), however, the equivalent number of bounces required is much less (~ 100), and the fractional power lost in the arms is a few percent or less. In this case, a power gain of ~ 30 is realistic. For fixed-mirror losses, the power lost in a cavity is inversely proportional to the input-mirror transmission, so the recycling gain is an optimally designed interferometer scales with the arm length, L_{arm}. Thus the increase in position sensitivity that is possible with power recycling scales as $(L_{arm})^{1/2}$.

The servo and signal detection schemes used here are convenient for this type of prototype experiment. Other techniques, such as using rf phase modulation to obtain the cavity-error signals, are possible and might be more appropriate for a full-scale interferometer.

Some comments about the losses in a large system can be made. The cavity finesse in this experiment is appropriate to a full-scale interferometer, but the coating technology has improved and (small) mirrors with a loss up to 10 times less than those used in this experiment are now available. Significant further reductions in the loss could be made by using a Michelson beam splitter and a recycling mirror made with low-loss coatings, and by using V coatings for all antireflection surfaces. The small contrast defect is not a significant loss in this experiment, but the beam is small ($\omega_0 \approx 0.3$ mm) compared with a full-scale system ($\omega_0 \approx 3$ cm). Because the phase-front distortions caused by the optical elements will be different on these two scales, we can make no conclusions about the contrast in a large system. Nonetheless, if the contrast is not less than $C \approx 0.99$, a power gain of at least 30 should be possible.

The vastly different recycling and arm-cavity lengths in a full-scale system produce a mode structure much different from this prototype, but this structure does not present any fundamental problems. For an arm length of 4 km and a recycling gain of ~ 30, the combined cavity linewidth of such a system is $\Delta\upsilon_{rec} \sim 5$Hz; see approximation (8). This linewidth will serve to filter the laser frequency and amplitude fluctuations in the gravity wave band.

VII. Conclusions

We have demonstrated the power recycling of a Michelson interferometer with Fabry–Perot cavity arms and an external modulation scheme for extracting the Michelson signal. The measured increase in power and in signal sensitivity for this system is a factor of 18, which agrees well with the expected gain given the known losses in the system.

We have also investigated some of the complexities of the resonance properties of a recycled Fabry–Perot arm Michelson interferometer. This investigation provide useful information in the designing of the modulation and servo systems of a full-scale interferometer.

This work is supported by National Science Foundation grant PHY-8803557.

We thank the entire LIGO team at Caltech and MIT for its support and collaboration.

References and Notes

1. D. Shoemaker, R. Schilling, L. Schnupp, W. Winkler, K. Maischberger, and A. Rüdiger, "Noise behavior of the Garching 30-meter prototype gravitational-wave detector," Phys. Rev. D **38,** 423–432 (1988).
2. R. Drever, "Interferometric detectors for gravitational radiation," in *Gravitational Radiation, Les Houches 1982,* N. Deruelle and T. Piran, eds. (North-Holland, Amsterdam, 1983), pp. 321–338.
3. J. Y. Vinet, B. Meers, C. N. Man, and A. Brillet, "Optimization of long-baseline optical interferometers for gravitational-wave detection," Phys. Rev. D **38,** 433–447 (1988).
4. B. J. Meers, "Recycling in laser-interferometric gravitational-wave detectors," Phys. Rev. D **38,** 2317–2326 (1988).
5. B. J. Meers, "The frequency response of interferometric gravitational wave detectors," Phys. Lett. A **142,** 465–470 (1989).
6. C. N. Man, D. Shoemaker, M. Pham Tu and D. Dewey, External modulation technique for sensitive interferometric detection of displacements, Phys. Lett. A **148,** 8–16 (1990).
7. K. A. Strain and B. J. Meers, "Experimental demonstration of dual recycling for interferometric gravitational-wave detectors," Phys. Rev. Lett. **66,** 1391–1394 (1991).
8. R. Vogt, "The U.S. LIGO project," presented at the Sixth Marcel Grossman Meeting on General Relativity, Kyoto, Japan, 23 June 1991.
9. R. Weiss, "Electromagnetically coupled broadband gravitational antenna," Mass. Inst. Technol. Res. Lab. Electron. Q. Rep. **105,** 54–76 (1972).
10. C. Townes and A. Schawlow, *Microwave Spectroscopy* (McGraw-Hill, New York, 1955), p. 426, in the context of microwave spectroscopy; proposed in the present context by R. Drever, California Institute of Technology, Pasadena, Calif. 91125 (personal communication, 1986).
11. D. Shoemaker, P. Fritschel, J. Giaime, N. Christensen, and R. Weiss, "Prototype Michelson interferometer with Fabry–Perot cavities," App. Opt. **30,** 3133–3138 (1991).
12. R. Schilling and L. Schnupp, Max-Planck Institut für Quantenoptik, Garching bei München, Germany (personal communication, 1986).
13. A. E. Siegman, *Lasers* (University Science, Mill Valley, Calif., 1986), pp. 524–530.